

Research Paper

Altered Expression of PERK Receptor Kinases in *Arabidopsis* Leads to Changes in Growth and Floral Organ Formation

Yosr Z. Haffani^{†,a}

Nancy F. Silva-Gagliardi^{†,b}

Sarah K. Sewter[†]

May Grace Aldea

Zhiying Zhao^d

Alina Nakhamchik^c

Robin K. Cameron^e

Daphne R. Goring^{*}

Department of Cell and Systems Biology; University of Toronto; Toronto, Ontario, Canada

Present addresses: ^aProgram in Molecular Biology and Cancer; Samuel Lunenfeld Research Institute; Mount Sinai Hospital; Toronto, Ontario, Canada; ^bThe Arthur and Sonia Labatt Brain Tumor Research Centre; The Hospital for Sick Children; Toronto, Ontario, Canada; ^cSunnybrook & Women's College Health Sciences Center; Toronto, Ontario, Canada; ^dCeres Inc.; Thousand Oaks, California USA; ^eDepartment of Biology; McMaster University; Hamilton, Ontario, Canada

[†]These authors contributed equally to this paper.

*Correspondence to: Daphne Goring; Department of Cell and Systems Biology; University of Toronto; 25 Willcocks Street; Toronto, Ontario M5S 3B2 Canada; Tel.: 416.978.2378; Fax: 416.978.5878; Email: d.goring@utoronto.ca

Received 07/17/06; Accepted 08/16/06

Previously published online as a *Plant Signaling & Behavior* E-publication: <http://www.landesbioscience.com/journals/psb/abstract.php?id=3324>

KEY WORDS

Arabidopsis, PERK, proline-rich extensin-like receptor kinase, cell wall, growth

ABBREVIATIONS

PERK proline-rich, extensin-like receptor kinase
WAK wall-associated receptor kinase

ACKNOWLEDGEMENTS

See page 259.

ABSTRACT

The proline-rich, extensin-like receptor kinase (PERK) family is characterized by a putative extracellular domain related to cell wall proteins, followed by a transmembrane domain and kinase domain. The original member, PERK1, was isolated from *Brassica napus* (*BnPERK1*) and 15 PERK1-related members were subsequently identified in the *Arabidopsis thaliana* genome. Ectopic expression and antisense suppression studies were performed using the *BnPERK1* cDNA under the control of the 35S CaMV constitutive promoter and introduced into *Arabidopsis*. In the case of antisense suppression, the *BnPERK1* cDNA shared sufficient sequence similarity to suppress several members of the AtPERK family. In both sets of transgenic *Arabidopsis*, several heritable changes in growth and development were observed. Antisense *BnPERK1* transgenic *Arabidopsis* showed various growth defects including loss of apical dominance, increased secondary branching, and floral organ defects. In contrast, *Arabidopsis* plants ectopically expressing *BnPERK1* displayed a prolonged lifespan with increased lateral shoot production and seed set. Along with these phenotypic changes, aberrant deposits of callose and cellulose were also observed, suggestive of cell wall changes as a consequence of altered PERK expression.

INTRODUCTION

Plants contain a large and diverse family of receptor kinases that play fundamental roles in various cellular processes.^{1,2} The receptor kinase family comprises the largest receptor family in plants with over 600 predicted genes in the *Arabidopsis* genome and over 1200 predicted genes in the rice genome.³⁻⁶ The putative extracellular domains of plant receptor kinases exhibit a range of different motifs, which may enable them to selectively respond to diverse extracellular signals. Plant receptor kinases are also unique in eukaryotes in terms of their domain organizations with assorted putative extracellular domains fused to a transmembrane domain, and a common ancestral serine/threonine kinase domain.³⁻⁶ Given the large number of plant receptor kinases, evidence of functional overlap between closely related members has started to emerge with examples including the *Arabidopsis* CLV1, BRI1 and ERECTA receptor kinases.⁷⁻¹¹

A number of biological functions for plant receptor kinases encompass roles as important regulators in plant development. Better known examples include the *Arabidopsis* BRI1 and BAK1 receptor kinases involved in the perception of brassinosteroids;¹²⁻¹⁴ the *Arabidopsis* CLV1 receptor kinase in the regulation of meristem differentiation;¹⁵ and the *Brassica S* receptor kinase in the rejection of self-incompatible pollen.¹⁶ Plant receptor kinases are also involved in plant-microbe interactions with the legume LRR and LysM receptor kinases required for symbiosis,¹⁷⁻²¹ while the rice Xa21 and *Arabidopsis* FLS2 receptor kinases activate pathogen defense responses.^{22,23}

A unique feature of plant receptor kinases is that they function within the constraints imposed by the presence of the cell wall, a dynamic structure composed of a complex network of carbohydrates and proteins. The plant cell wall plays a pivotal role in the modulation of plant growth and development as well as mediating interactions with the external environment.^{24,25} Several putative plant receptor kinase classes have been found to contain motifs in the putative extracellular domains related to cell wall proteins or implicated in carbohydrate binding suggesting that these putative receptor kinases may have close associations with cell wall components.⁴ A tight association with the cell wall has been biochemically-demonstrated for the *Arabidopsis* Wall-Associated receptor Kinase1.²⁶ Moreover, WAK1 is known to bind cell wall pectins, and have a role in cell expansion, potentially through the regulation of turgor.²⁷⁻³⁰

The *Arabidopsis* PERKs make up one of the smaller receptor-like kinase families with 15 members and share a putative extracellular domain related to cell wall proteins.^{3,31} The predicted PERK extracellular domains are rich in proline residues and contain multiple copies of Ser(Pro)_x, a motif found in hydroxyproline-rich glycoproteins such as the extensin family of cell wall proteins.³¹⁻³³ Cell wall proteins form structural networks in the plant cell wall and play important roles in the strength and assembly of cell walls.³² Analyses of cell wall protein mutants are also starting to reveal more precise functions for individual cell wall proteins. For example, *Arabidopsis* LRR extensins, LRX1 and 2, have been found to be required for proper formation of the cell wall in root hairs, and the hydroxyproline-rich glycoprotein, RSH, is required for proper embryo development.^{34,35} We previously reported the characterization of a putative receptor kinase from *Brassica napus* designated PERK1 (proline-rich extensin-like receptor kinase 1). *BnPERK1* was found to be ubiquitously expressed, and mRNA levels rapidly increased in response to wounding.³³ In *Arabidopsis*, there are 15 predicted members sharing a putative related proline-rich extracellular domain. The expression patterns of the *AtPERK* family members fall into two broad classes with several members highly expressed in pollen while other members are more broadly expressed.³¹ Here, we investigate the role of PERKs during *Arabidopsis* growth using ectopic expression and antisense suppression approaches. Ectopically-expressing *BnPERK1* transgenic *Arabidopsis* plants were found to display an enhanced growth phenotype while antisense-suppressed PERK transgenic *Arabidopsis* plants were found to have altered growth and abnormal flowers.

MATERIALS AND METHODS

Plant material, growth conditions and plant transformations. Wild-type and transgenic seeds were surface sterilized in 70% ethanol for 5 min followed by a 15 min wash in 20% (v/v) bleach with 0.05% Tween-20. Seeds were rinsed five to six times with sterile water. All seeds were then kept in the dark at 4°C in water for 1 to 4 days to synchronize germination. Seeds were germinated on media containing 0.5X Murashige and Skoog salts (Gibco BRL), 2.5 mM morpholino ethane sulfonic acid (MES, Sigma), and 1% (w/v) phytagar at pH 5.7 in a growth chamber at 23°C under a 16 hour light/8 hour dark cycle, or directly sown on soil. Plants grown in soil were placed in a growth chamber maintained at 22°C with a 16 hour light/8 hour dark cycle and a humidity level of 70–80%. For growth measurements on the ectopic *BnPERK1* transgenic *Arabidopsis*, plants were maintained at 22°C under 16 hour light/8 hour dark cycle with a light intensity of 100–120 $\mu\text{Ein}/\mu\text{s}^2$. For root growth in liquid media, seedlings were grown in liquid 0.5 X MS minimal media buffered with 500 mM MES pH 5.7.

The full-length *BnPERK1* cDNA was cloned in the sense and antisense orientation next to the CaMV 35S promoter in pBI221 (Clontech). The CaMV 35S-*BnPERK1*-Nos terminator cassettes were subsequently digested as *HindIII*-*EcoRI* fragments, cloned into the pCAMBIA 2301 plant transformation vector (CAMBIA), and used for transforming *Arabidopsis thaliana* Col-0. For the *BnPERK1*-HA construct used for protein localization, the full length *BnPERK1* coding region was amplified with gene-specific primers and the HA epitope sequence (YPYDVPDVA) incorporated into the reverse primer, and cloned into the pBI221 as a *Bam*HI-*Sac*I fragment. The resulting CaMV 35S-*BnPERK1*-HA-Nos terminator cassette was subsequently transferred into pCAMBIA 2301 as a *HindIII*-*EcoRI* fragment, and used for transforming *Arabidopsis thaliana* Ws-2.

For the construction of *AtPERK1*, 2, and 3 promoter::GUS fusions, TAIR (<http://www.Arabidopsis.org/>), TIGR (<http://www.tigr.org/tdb/e2k1/ath1/>), and MIPS (<http://mips.gsf.de/proj/thal/db/>) databases were used to determine the locations of these genes on the chromosome. The predicted promoter regions (*AtPERK1*: 2800 bp; *AtPERK2*: 1289 bp; *AtPERK3*: 2044 bp) were amplified by PCR with the forward primer designed to anneal following the stop codon of the previous gene and the reverse primer designed to anneal before the start codon of the *AtPERK* gene. *AtPERK2* and 3 primers included *EcoRI* restriction sites while *AtPERK1* primers had *Pst*I and *Bam*HI restriction sites for cloning into TOPO pCR 2.1 (Invitrogen). All positive clones were sequenced to confirm their identity (York University Core Molecular Biology and DNA Sequencing Facility, Toronto), and transferred into the binary vector pCAMBIA 1391Z (CAMBIA) to create the promoter::GUS transcriptional fusions for transformation into *Arabidopsis thaliana* Col-0.

All pCAMBIA constructs were transferred to *Agrobacterium tumefaciens* GV3101, and plant transformations were performed following the floral dip method described by Clough and Bent.³⁶ Transgenic plants were selected on 0.5 x MS minimal media supplemented with 50 mg/L kanamycin for pCAMBIA 2301, or on basal media containing 1 mM potassium nitrate, 50 $\mu\text{g}/\text{mL}$ hygromycin, and 25 $\mu\text{g}/\text{mL}$ carbenicillin, at pH 5.7³⁷ for pCAMBIA 1391Z, and then propagated on soil for further analysis. Final analyses on the ectopic and antisense suppressing *PERK* transgenic lines were performed on T2 - T4 generations. T₁ to T₃ generation plants from at least two independent lines were characterized for the *AtPERK1* and *AtPERK3* promoter::GUS lines.

RNA isolation and RNA blot analysis. Total RNA was isolated from rosette leaf tissue, flowers or roots as described by Cock et al.³⁸ Ten micrograms of total RNA was fractionated on a 1.2% (w/v) formaldehyde gel, transferred onto Hybond N⁺ membrane (Amersham Pharmacia) and transferred in 10 X SSC. Hybridization was performed with either the full length *BnPERK1* cDNA, or the putative extracellular domains of *AtPERK6*, 7, 8, 9, 10 and 13 cDNAs, respectively.³¹ High-stringency wash conditions were conducted with a final wash 0.1 X SSC, 0.1% SDS for 20 min at 65°C. The blots were subjected to autoradiography (XAR-5 film, Kodak) at -80°C for two days.

For *AtPERK1*, 2 and 3, single-stranded riboprobes were used. The putative extracellular domain regions from *AtPERK1*, 2 and 3 cDNAs were cloned into pBluescript KS⁺ (Stratagene) in the antisense orientation under the control of T7 promoter. Single-stranded antisense *AtPERK1*, 2 and 3 transcripts were synthesized in-vitro and labeled with [γ -³²P]dUTP using the MAXIscript™ kit (Ambion), as recommended by the manufacturer. Labelled riboprobes were separated from unincorporated nucleotides using MicroSpin G-25 columns (Amersham Pharmacia Biotech). The riboprobes were hybridized to filters overnight at 68°C. Filters were then washed extensively, with a final wash at 68°C in 0.1% SDS and 0.1 X SSC.

Preparation of plant protein extracts and Western blot analyses. Total protein extracts were prepared from leaf tissue of four week-old *BnPERK1*-HA transgenic and wild-type *Arabidopsis* plants. The tissue was ground with liquid nitrogen and extracted in a homogenization buffer [10 mM Tris-HCl, pH 7.3, 150 mM NaCl, 1 mM EDTA, 10% (w/v) glycerol, 1% (w/v) Triton X-100, 1 mM PMSF and Complete mini proteinase inhibitor tablets (Boehringer-Mannheim)].¹³ The lysate was placed on a nutator and allowed to solubilize for 2 h at 4°C, followed by a final centrifugation for 15 min at 16,000 g. The protein concentrations were determined using Bradford reagent (BioRad) and BSA as a standard.

For the aqueous two-phase partitioning, microsomal membrane fractions were prepared from 16 g of leaf tissue. The tissue was homogenized with a mortar and pestle using quartz sand and the homogenization buffer [30 mM Tris-HCl, pH 7.5, 2 mM EDTA, 250 mM mannitol, 10% (w/v) glycerol, 1 mM PMSF, 5% (w/v) insoluble PVP, Complete mini proteinase inhibitor tablets (Boehringer-Mannheim)]. After filtration through eight layers of Miracloth (Calbiochem), the homogenate was centrifuged at 2000 g for 10 min at 4°C. The supernatant was removed and centrifuged at 8000 g, 4°C for 20 min, and then recentrifuged in a Ti60 rotor (Beckman) at 100,000 g for 45 min. The resulting supernatant represented the soluble fraction, and the resulting pellet represented the microsomal membrane fraction which was resuspended in 1 ml of storage buffer [6 mM Tris-HCl, pH 7.5, 10% (w/v) glycerol, 250 mM mannitol, 1 mM DTT, 1mM PMSF, and complete mini proteinase inhibitor tablets (Boehringer-Mannheim)]. The microsomal membrane fraction was then subjected to two-phase partitioning to enrich for plasma membrane as described by Larsson et al.³⁹ The resulting lower and upper phases were aliquoted and stored at -80°C.

Protein samples were separated through an 8% SDS-PAGE gel and electroblotted onto nitrocellulose membrane (Osmonics Inc.). The membranes were blocked for 1 h at room temperature in PBS-T (137 mM NaCl, 2.7 mM KCl, 4.3 mM Na₂PO₄, 0.1% Tween-20) with 5% (w/v) nonfat dried milk. Primary antiserum incubations were performed in PBS-T with 5% (w/v) nonfat dried milk overnight at 4°C according to the following dilutions: the high affinity monoclonal HA3F10 antiserum (Roche Diagnostics; 1:2000–1:4000); H⁺-ATPase (1:3000). Secondary antiserum incubations were performed for 2 h at room temperature and diluted as follows: goat anti-rat horseradish peroxidase-conjugated IgG (1:4000–1:8000) (Chemicon International.); goat anti-rabbit horseradish peroxidase-conjugated IgG (1:5000) (Kirkegaard & Perry Laboratories), followed by four washes of 15 min in PBS-T. Chemiluminescence detection was performed with the LumiGlo substrate kit according to the manufacturer's recommendations (Kirkegaard & Perry Laboratories).

Morphological characterization. Transgenic lines with wild-type controls were characterized as follows: plant height was determined by measuring the length of the longest inflorescence. For the number of ovules per pistil, flowers were obtained from plants of the same age and growth conditions. Twenty pistils were cleared and stained with aniline blue as described in Stone et al.⁴⁰ Ovules were counted per individual ovary under the fluorescence microscope. For the number of seeds per silique, siliques were collected from fully mature plants (55 to 60 days old).

To examine hypocotyl elongation of dark-grown seedlings, seeds were plated on minimal media as described above, and plates were placed in the dark at 23°C for 6–7 days. Hypocotyls were measured with a ruler under a light-dissecting microscope with 70 to 170 hypocotyls measured for each line. For hypocotyl epidermal cell lengths, hypocotyls were fixed in 70% ethanol and cleared in chloral hydrate:glycerol:water (8:2:1, w/v/v). Digital images were taken with the light microscope and measured for length using the Northern Eclipse Image software. For each line, 15 to 65 epidermal cells from 5 to 7 hypocotyls were measured.

For the root elongation assay, seedlings were initially grown for two days on 0.3% Agar minimal medium supplemented with kanamycin 50 mg/L under light and temperature as described above. Fifteen germinated seedlings were then transferred and aligned in a large petri dish (180 mm) containing 3% agar minimal

medium supplemented with 50 mg/L kanamycin. Root tips of the aligned seedlings were marked at the bottom of the Petri dish and then used as a starting root elongation line. All plates were placed vertically to allow the roots to grow along the surface of the minimal medium. Root elongation was measured in 12 hour intervals for up to 14 days, and development was scored according to Lincoln et al.⁴¹

Fluorescence and confocal laser scanning microscopy. Callose was detected with Aniline Blue (Sigma) resuspended at 0.1 mg/ml in phosphate buffer pH 9.0; cellulose was detected with Calcofluor White M2R dye (Sigma) resuspended at 0.1 mg/ml in phosphate buffer pH 7.0; and lignin was detected with phloroglucinol using a saturated solution in 20% hydrochloric acid. Five day-old seedlings, and pistils from freshly opened flowers were used. Fluorescence microscopy (Axioskop, Zeiss) was used to monitor the callose, cellulose and lignin deposition. Cellulose deposition was also visualized using confocal laser scanning microscopy (BioRad).

Detection of GUS activity and microscopy. At least two independent transformed lines were tested for each of the promoter::GUS constructs. Plant tissues from the *AtPERK* promoter::GUS transgenic lines were stained for GUS activity following incubation in 100 mM NaPO₄ pH 7.0, 10 mM EDTA, 0.5 mM potassium ferricyanide, 0.5 mM potassium ferrocyanide, 0.1% Triton X-100, 1.9 mM X-gluc, and 20% (v/v) methanol, or following protocols in Shi et al.⁴² and Kang and Dengler.⁴³ The GUS substrate, 1.9 mM 5-bromo-4-chloro-3-indolyl-β-D-glucuronic acid, was purchased from BioVectra (Charlottetown, PEI, Canada), and incubation times ranged from 30 minutes to overnight at 37°C. Vacuum infiltration of 10 to 15 minutes was also used for some samples to increase the rate at which the blue color appeared. Siliques were opened longitudinally along the valve with forceps to facilitate substrate penetration. After staining, samples were taken through several changes of 70% ethanol to remove chlorophyll, hydrated in distilled water, and further cleared in chloral hydrate:glycerol:water (8:2:1, w/v/v) for at least three days before mounting on slides. Digital images of the samples were obtained using a Leica MZ FLIII dissecting microscope, by light and dark-field optics on a Leica stereomicroscope, or under differential interference contrast (DIC) on a Reichert-Jung Polyvar microscope.

RESULTS

To begin to explore the biological functions of the PERK family, ectopic expression and antisense suppression studies were conducted in *Arabidopsis thaliana* Col-0. For these experiments, the full length *BnPERK1* cDNA was placed in both directions under the control of the strong, constitutive CaMV 35S promoter. The *Arabidopsis* PERK family is comprised of 15 members, and based on a phylogenetic analysis, *BnPERK1* is most closely related to *AtPERK1*.³³ Thus, *BnPERK1* appears to be the orthologue of *AtPERK1*, with 84% nucleotide sequence identity and 88% amino acid sequence identity (Fig. 1A). More importantly, this similarity includes a highly conserved domain organization with a putative proline-rich extracellular domain of approximately 135 amino acids in length (which varies for other family members), followed by a highly similar transmembrane domain, a second short proline-rich juxtamembrane domain and kinase domain (92% amino acid identity) (Fig. 1A). The *BnPERK1* and *AtPERK* proteins do not have predicted signal sequences at the N-terminus, but follow the predicted 'positive-inside' rule where the cytosolic kinase domain has a region enriched in arginine and lysine residues adjacent to the transmembrane domain⁴⁴ (Fig. 1A). Finally, *BnPERK* and *AtPERK1* share similar patterns of expression.^{31,33}

The *BnPERK1* cDNA also shares significant nucleotide sequence identity to other *AtPERK* family members which could potentially lead to antisense suppression of several *AtPERK* members. There is a 600 bp region in the kinase domain that is highly conserved in *AtPERK1* -3 (85–91% DNA sequence identity; Fig. 1B), and moderately conserved in the rest of the *AtPERK* members (68–74% DNA sequence identity; Fig. 1B). Given these levels of sequence similarity, all of the *AtPERK* genes could potentially be subject to some degree of antisense RNA suppression by the *BnPERK1* transgene. Transgenic seedlings carrying either the ectopic or antisense *BnPERK1* constructs were identified as kanamycin resistant and grown to the next generation for further analyses. Experiments were conducted in either the T₃ or T₄ generations for the ectopic lines, or T₂ generation for the antisense plants.

Analysis of the ectopic *BnPERK1* transgenic arabidopsis. RNA blot analysis of leaf mRNA was conducted to screen for transgenic *Arabidopsis* lines ectopically expressing *BnPERK1* and resulted in the identification of three independent transgenic lines (S2, S4 and S10) that exhibited high levels of the *BnPERK1* transcript in the leaves (Fig. 2A). These lines were found to carry a single copy of the transgene as determined by genomic Southern blot analysis (data not shown). Transgenic plants using a C-terminal HA epitope tag to detect the *BnPERK1* protein were tested to determine if the ectopically expressed *BnPERK1* was localized to the plasma membrane, as predicted (Fig. 2B). Aqueous two-phase partitioning was used to purify plasma membrane from leaf tissues of the transgenic *Arabidopsis*, and *BnPERK1*-HA was assayed in the soluble (S), lower (L), and upper (U) phase fractions. *BnPERK1*-HA was predominantly detected in the upper phase fraction corresponding to the enriched plasma membrane along with the H⁺-ATPase plasma membrane control marker, which is consistent with *BnPERK1* localization to the plasma membrane (Fig. 2B). The *BnPERK1*-HA signal was completely absent as expected from the soluble fraction representing concentrated cytosolic (soluble) proteins (Fig. 2B), and in two-phase fractions prepared from nontransgenic *Arabidopsis* plants (data not shown).

Phenotypic changes in growth for the ectopic *BnPERK1* transgenic arabidopsis. Initial observations of the S2, S4 and S10 ectopic *BnPERK1* *Arabidopsis* lines suggested that these plants showed increased growth when compared to wild-type *Arabidopsis*. These results were most pronounced when these transgenic plants were grown under reduced lighting conditions. As a result, these plants were examined more closely for phenotypic alterations during growth and development under lower light conditions. The initial stages of growth following germination were similar to wild-type *Arabidopsis*. In terms of root growth, the S2, S4 and S10 ectopic

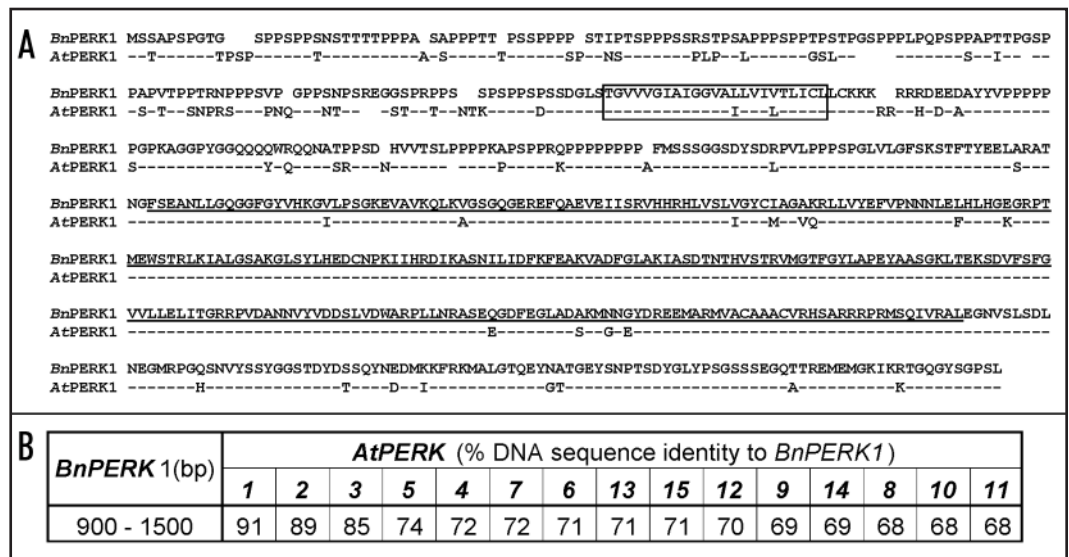


Figure 1. Sequence identity between the *BnPERK1* and the *AtPERK* family. (A) Amino acid sequence alignment of *BnPERK1* and *AtPERK1*. The high degree of sequence identity as well as conserved domain organization between *BnPERK1* and *AtPERK1* is observed throughout the amino acid sequence. Identical amino acids are denoted by hyphens, and spaces represent gaps in the alignment. The predicted transmembrane domain is boxed, and the catalytic kinase domain is underlined. (B) Nucleotide sequence identity between *BnPERK1* and *AtPERKs* in a highly conserved region in the kinase domain.

BnPERK1 *Arabidopsis* lines did not show any obvious differences in comparison to wild-type *Arabidopsis*, both in terms of morphology and root growth rates. There was also no significant difference with respect to bolting and flowering times between wild-type and ectopic *BnPERK1* transgenic *Arabidopsis*. However, the S2, S4 and S10 lines did show some changes in senescence, seed production, height, secondary branching, and generally had a prolonged lifespan compared to wild-type *Arabidopsis* (Table 1). The transgenic plants were harvested at two different time points, 60 and 82 days. Whereas wild-type *Arabidopsis* had already reached senescence at 82 days, the transgenic lines typically continued to produce additional lateral shoots and flowers at 60 days, and were still producing some flowers at 82 days following germination. The increased height was somewhat variable with a significant increase seen only for the S4 line when the transgenic plants were harvested at 60 days, and for the S10 line in both trials (Table 1).

Interestingly, there was a significant increase in the number of ovules per pistil and seeds per silique associated with the ectopic expression of *BnPERK1* (Table 1; Fig. 3A). In the case of the S2 and S10 lines, this was associated with an increase in the average dry seed weight produced per plant. The S4 line did not show this increase in dry seed weight, but appeared to produce fewer flowers. During the analyses of the number of ovules in the pistils of the ectopic *BnPERK1* transgenic plants (S2, S4 and S10), it was observed that there were aberrant callose deposits in these transgenic lines. The callose deposition in the ovules of the ectopic *BnPERK1* transgenic plants was detected by staining with aniline blue, followed by fluorescence microscopy (Fig. 3C). This was not observed in wild-type ovules from *Arabidopsis* (Fig. 3B) plants.

Analysis of the antisense *BnPERK1* transgenic arabidopsis. For the antisense suppression of endogenous *AtPERK* genes, a number of independent transformed plants were recovered and defects in growth were observed. Four independent antisense *BnPERK1* transgenic *Arabidopsis* lines, AS1, AS2, AS35 and AS37, were grown

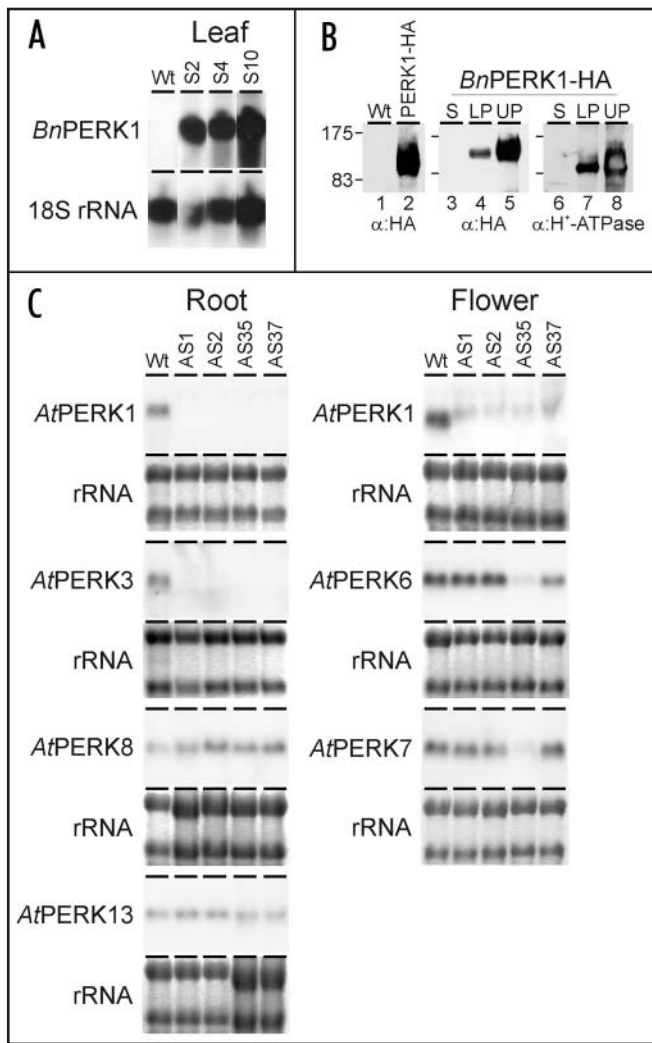


Figure 2. Expression analysis of the ectopic and antisense *BnPERK1* transgenic *Arabidopsis*. (A) RNA blot analysis of the ectopic expression of *BnPERK1* in three independent *Arabidopsis* lines, S2, S4 and S10. Five micrograms of total RNA was loaded and the blot was probed with full length *BnPERK1* cDNA and subsequently reprobed with the 18S rRNA DNA as a control for loading. Each blot was repeated at least twice and a representative image is shown. (B) Ectopically expressed *BnPERK1*-HA is localized to the plasma membrane. Lane 1-2: Total leaf protein extracts from wild-type (lane 1) and ectopic *BnPERK1*-HA plants (lane 2), subjected to western blot analysis using a monoclonal HA antibody. A clear band is detected in total leaf extracts from the ectopic *BnPERK1*-HA plants (lane 2). Lane 3-8: Total protein lysates prepared from leaf tissue were fractionated into the soluble fraction (S), and the total microsomal membrane fraction which was then further fractionated by aqueous two-phase partitioning into lower (LP) and upper phases (UP), corresponding to the endomembrane and plasma membrane enriched fractions respectively. Each lane contains 5 μ g of each fraction, and were subjected to Western blot analysis using either the HA antibody (lanes 3-5) or a control antibody against the plasma membrane H^+ -ATPase (lane 6-8). Both antibodies detect a strong band in the plasma membrane enriched upper phase (lanes 5 and 8). (C) RNA blot analysis of the antisense *BnPERK1* transgenic lines, AS1, AS2, AS35, and AS37. Ten micrograms of total RNA was loaded in each lane, and blots were hybridized with *AtPERK1* and 3 riboprobes (putative extracellular domain only), and *AtPERK6*, 7, 8 and 13 cDNAs. Ethidium bromide stains of the rRNAs for each blot are shown as a control for loading.

and analyzed in more detail. RNA blot analyses were conducted to determine which *AtPERK* genes were suppressed in these lines. Two different tissues, root and flower buds, were tested with a subset of *AtPERK* genes that were known to be expressed in these tissues.³¹ *AtPERK1*, 3, 8 and 13 were tested for expression in the root, and *AtPERK1*, 6 and 7 were tested for expression in flower buds (Fig. 2C). *AtPERK1* and 8 are expressed throughout the plant at relatively high levels, while *AtPERK3* is expressed at very low levels in the root and flower bud, and *AtPERK13* exhibits root-specific expression.³¹ *AtPERK6* and 7 have flower bud-specific expression patterns, which in fact appear to be pollen-specific when examined more closely in the AtGenExpress microarray database.^{31,45}

For all four lines, *AtPERK1* and 3 expression was suppressed in roots while *AtPERK8* expression was not. In the case of flower buds, *AtPERK1* was suppressed in all four lines and *AtPERK6* and 7 were suppressed in only the AS35 line. *AtPERK6* mRNA levels were slightly reduced in AS37 as well (Fig. 2C). Thus, consistent RNA suppression was observed with *AtPERK* genes most closely related to *BnPERK1*, while more variable or no suppression was observed with more distantly related *AtPERK* genes (Fig. 1B and Fig. 2C). *AtPERK2* is a third gene closely related to *AtPERK1* and 3, but we were unable to verify its suppression. *AtPERK2* mRNA could not be detected in wild-type *Arabidopsis* using RNA blot analysis with an *AtPERK2*-specific riboprobe or RT-PCR (data not shown). While we had previously reported *AtPERK2* expression in flower buds and siliques, this signal may have resulted from some cross-hybridization to other closely related *AtPERK* mRNAs.³¹ This is also supported by the complete absence of detectable *AtPERK2* expression in all tissues and treatments examined in the AtGenExpress microarray database.⁴⁵

In comparison to wild-type *Arabidopsis*, the mature transgenic plants in all four lines exhibited shorter stems and reduced apical dominance, while the leaves remained unaffected (Fig. 3D). In terms of root growth, the AS1 and AS2 antisense lines produced roots that were similar in growth to wild-type plants. The AS35 and AS37 antisense lines were more variable with some of the seedlings producing shorter primary roots, and in 5-10% of these seedlings, the short primary root showed radial swelling with disruptions of the root cell layers. This was not observed in wild-type *Arabidopsis* grown for comparison.

The four antisense *BnPERK1* transgenic *Arabidopsis* lines produced flowers that were often abnormal in shape and reduced in fertility (Fig. 3E). The AS1 and AS2 lines had a less severe phenotype, in comparison to AS35 and AS37, and produced a larger number of floral buds. Approximately 70% of the AS1 and AS2 flowers were generally similar in appearance to wild-type flowers while the remaining AS1 and AS2 flowers were often abnormal in shape with the presence of a second carpel-like structure (Fig. 3G). The AS1 and AS2 flowers also had reduced fertility resulting in decreased number of seeds per siliques (Fig. 3K). Seed yields from AS1 and AS2 were roughly 10-30% less when compared to wild-type *Arabidopsis*. The AS35 and AS37 plants also flowered but produced few viable seeds with approximately 10 to 100 seeds/plant. The AS35 line, and to a lesser extent the AS37 line, had very few wild-type flowers and produced an increased number of defective flowers compared to the AS1 and AS2 lines (Fig. 3H and I). The floral organ defects and reduced fertility were observed in the antisense *BnPERK1* transgenic *Arabidopsis* lines throughout flowering, but not in the control wild-type *Arabidopsis* grown simultaneously.

Hypocotyl growth in the ectopic and antisense *BnPERK1* transgenic *Arabidopsis*. To examine if cell expansion was affected in the

Table 1 **Growth Characteristics of the Ectopic *BnPERK1* transgenic *Arabidopsis***

| | | Col-0 | S2 | S4 | S10 |
|--|---|------------------------------|-------------------------------|--------------------------------|--------------------------------------|
| Average ovules/pistil (\pm SE) | 1 | 42.39 \pm 1.17 (n = 28) | nd | 55.71 \pm 1.17* (n = 17) | 53.27 \pm 1.58* (n = 22) |
| | 2 | 40.64 \pm 1.30 (n = 14) | 54.12 \pm 1.34* (n = 17) | nd | 51.18 \pm 1.64* (n = 11) |
| Average seeds/silique (\pm SE) | 3 | 34.03 \pm 0.91 (n = 79) | nd | 46.59 \pm 0.62* (n = 152) | 48.38 \pm 0.74* (n = 135) |
| | 4 | 40.89 \pm 0.96 (n = 38) | 52.33 \pm 0.62* (n = 72) | 51.67 \pm 0.75* (n = 36) | 52 \pm 0.93* (n = 29) |
| Average dry seed mass (mg)/plant (\pm SE) | 3 | 127.1 \pm 17.4 (n = 17) | nd | 141.6 \pm 9.1 (n = 37) | 179.3 \pm 15.4* (n = 40) |
| | 4 | 147.9 \pm 20.4 (n = 19) | 343.9 \pm 44.6* (n = 21) | 147.5 \pm 25.6 (n = 49) | 206.1 \pm 33.9 (n = 37; P=0.07) |
| Average Height (cm) | 3 | 35.94 \pm 1.45 (n = 17) | nd | 47.83 \pm 0.65* (n = 41) | 45.15 \pm 0.84* (n = 40) |
| | 4 | 53.11 \pm 1.68 (n = 19) | 50.10 \pm 1.45 (n = 21) | 55.71 \pm 0.76 (n = 49) | 57.34 \pm 1.08* (n = 50) |
| Average # of lateral shoots/plant | 3 | 27.06 \pm 1.50 (n = 17) | nd | 31.38 \pm 1.63* (n = 40) | 43.05 \pm 2.00* (n = 40) |
| | 4 | 22.26 \pm 2.11 (n = 19) | 34.47 \pm 2.21* (n = 19) | 29.65 \pm 1.53* (n = 47) | 37.87 \pm 2.12* (n = 31) |

All values \pm standard error; nd, not determined; n = # of plants. *Denote averages with statistically significant differences relative to Col-0 (t-test, $p < 0.05$). Expt 1, 24 February 2003; Expt 2, 20 April 2003; Expt 3, October 2002—Harvested at Day 60 (Col-0 senescent, S4 and S10 still producing lateral shoots and flowering); Expt 4, July 2003—Harvested at Senescence day 82 (when Col-0 stopped flowering, S2, 4, 10 were still flowering).

ectopic and antisense *BnPERK1* transgenic *Arabidopsis*, hypocotyl growth was measured in dark grown seedlings for the three ectopic *BnPERK1* transgenic lines, S2, S4 and S10, and the four antisense

BnPERK1 transgenic lines, AS1, AS2, AS35, AS37. The S2, S4 and S10 hypocotyl lengths were significantly shorter than wild-type *Arabidopsis*. In contrast, three of the antisense lines, AS1, AS2 and AS35, displayed longer hypocotyls compared to wild-type *Arabidopsis* (Fig. 4A). The length of individual hypocotyl cells was also measured to investigate if there were any changes in hypocotyl cell size in relation to overall length. The S2, S4 and S10 lines had significantly shorter hypocotyl cells in comparison to wild-type *Arabidopsis*. The mild antisense *BnPERK1* transgenic lines, AS1 and AS2 had longer hypocotyl cells, whereas the stronger antisense *BnPERK1* transgenic lines, AS35 and AS37 showed little or no change in length in comparison to wild-type *Arabidopsis*. (Fig. 4B).

Accumulation of callose and cellulose in the ectopic and antisense *BnPERK1* transgenic *Arabidopsis*. During the

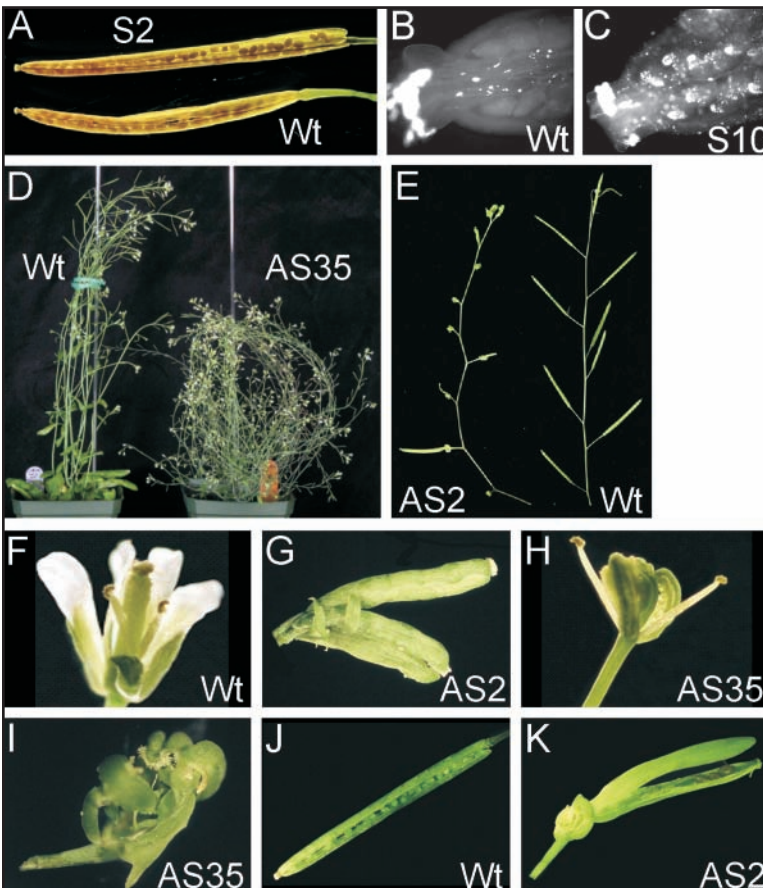


Figure 3. Phenotypic changes in the ectopic and antisense *BnPERK1* transgenic *Arabidopsis*. (A) Representative seed pods are shown from wild-type and the ectopic *BnPERK1* transgenic S2 line. An increase in the number of seeds per silique was observed in the ectopic *BnPERK1* transgenic lines when compared to wild-type Col-0. (B and C) Histochemical staining of callose with aniline blue in pistils from (B) Wild-type and (C) S10 plants. Increased callose deposits were observed in the ectopic *BnPERK1* transgenic pistils. (D and E) Antisense *BnPERK1* transgenic lines exhibited reduced height, loss of apical dominance, and partial sterility. Representative examples are shown for the (D) AS35 and (E) AS2 lines. (F–I) The antisense *BnPERK1* transgenic lines exhibited defective flowers. Flowers from (F) wild-type, (G) AS2, (H and I) AS35 are shown. The milder AS1 and AS2 lines showed approximately 30% abnormal flowers such as shown in (G). The strong AS35 and AS37 lines rarely had wild-type flowers and typically had abnormal flowers as shown in (H and I) throughout their life cycle. (J and K) Siliques from (J) wild-type and (K) AS2 plants. Siliques have been opened to show seeds. The antisense *BnPERK1* transgenic plants exhibited reduced seed production.

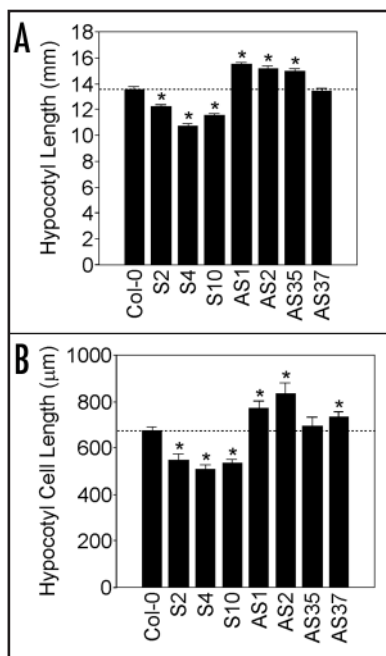


Figure 4. Hypocotyl length in the ectopic and antisense *BnPERK1* transgenic *Arabidopsis*. (A) Hypocotyl length and (B) hypocotyl cell length for dark grown seedlings from the ectopic *BnPERK1* S2, S4, and S10 lines and the antisense *BnPERK1* AS1, AS2, AS35 and AS37 lines. *Denote averages with statistically significant differences relative to Col-0 (t-test, $p < 0.05$).

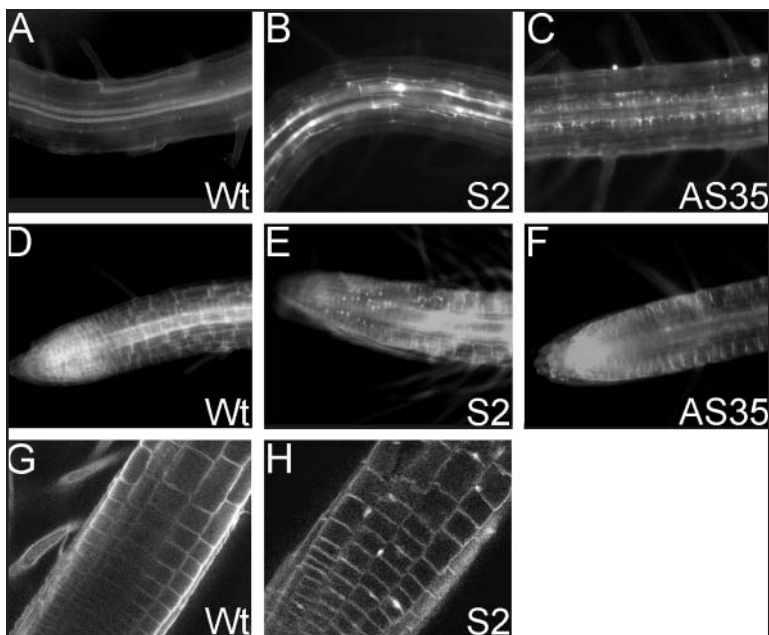


Figure 5. Callose and cellulose deposition in the ectopic and antisense *BnPERK1* transgenic *Arabidopsis*. (A to C) Histochemical staining of callose with aniline blue in roots from 5 day old seedlings. (A) Wild-type; (B) S2; and (C) AS35. (D to H) Histochemical staining of cellulose with calcofluor white M2R in roots from 5 day old seedlings. (D–G) Wild-type; (E–H) S2; and (F) AS35. A–F were visualized by widefield fluorescence microscopy while G–H were visualized by confocal IS fluorescence microscopy.

analyses of the ectopic *BnPERK1* transgenic plants for ovule numbers in the pistils, it was observed that there were increased callose deposits in these transgenic lines (Fig. 3C). To investigate if the callose

deposits were an indication of more generalized alterations in cell wall materials, roots from transgenic plants were examined for changes in callose, lignin, and cellulose deposition. Transgenic roots from ectopic and antisense *BnPERK1* transgenic *Arabidopsis* were examined for altered lignin deposition using a phloroglucinol stain; however, no abnormal lignin deposition was observed (data not shown). Transgenic roots were also examined for callose using an aniline blue stain. In comparison to wild-type *Arabidopsis* roots (Fig. 5A), aberrant callose deposits was observed in the ectopic *BnPERK1* transgenic roots (S2, S4 and S10) as shown for S2 roots (Fig. 5B), and in the antisense *BnPERK1* transgenic lines (AS1, AS2, AS35 and AS37) as shown for AS35 (Fig. 5C). The presence of these aberrant callose deposits was variable, and they were absent in some of the roots tested. Finally, transgenic roots were examined for cellulose deposition using a calcofluor white M2R stain. In comparison to wild-type *Arabidopsis* roots (Fig. 5D), aberrant deposits of cellulose were detected in the ectopic *BnPERK1* transgenic lines. For example, using fluorescence microscopy, aberrant cellulose deposits were observed in the S2 roots (Fig. 5E). The cellulose deposits were examined in more detail using confocal microscopy, and very small amorphous patches of cellulose were visualized in the cell walls as shown for S2 roots (Fig. 5H), in comparison to wild-type (Fig. 5G). For the antisense *BnPERK1* transgenic lines, cellulose deposits were not observed in the roots (Fig. 5F).

AtPERK promoter::GUS expression patterns. Given the range of defects observed with the strong suppression of the *AtPERK1* and 3 genes, their expression patterns were more closely examined through the analysis of *AtPERK1* and 3 promoter::GUS transgenic *Arabidopsis* (Fig. 6). *AtPERK2* promoter::GUS transgenic *Arabidopsis* were also generated, but again no expression could be detected, despite using a promoter fragment that included the entire 5' region up to the next gene. In general, *AtPERK1* promoter::GUS transgenic plants (Fig. 6A–J) showed much higher GUS activity levels relative to the *AtPERK3* promoter::GUS transgenic plants (Fig. 6K–O), consistent with our previous RNA blot analyses.³¹ In young seedlings carrying the *AtPERK1* promoter::GUS transgene, GUS activity was high in the vascular tissues of cotyledons, developing leaves, and lower throughout the cotyledons and in the hypocotyl (Fig. 6A–C). High GUS activity was also detected in all regions of the root, except the division zone that showed a complete absence of staining (Figs. 6A, C and D). Examination of lateral root primordia and emerging lateral roots revealed strong GUS activity in these areas (Fig. 6E). In mature *AtPERK1* promoter::GUS transgenic plants, moderate levels of GUS activity were also consistently observed in the vasculature of vegetative organs, including rosette and cauline leaves, and mature stems as well as in the hydathodes (Fig. 6F and G). Developmentally, the *AtPERK1* promoter appeared to be active in the vascular tissue of both newly developing and fully expanded leaves (data not shown and Fig 6F). Strong GUS staining was also seen in the vasculature of several parts of the flower, including sepals and stamen filaments (Fig. 6H and I) while less intense staining was observed in the vasculature of petals of open flowers (Fig. 6I). Finally, mature siliques also exhibited strong vascular staining, including in the funiculi (Fig. 6J).

The *AtPERK3* promoter::GUS transgenic plants generally had very weak GUS activity levels (Fig. 6K and O). In young seedlings, GUS activity was restricted to the hypocotyl, with more intense

activity apparent in the vasculature, and diffuse staining in adjacent cells (Fig. 6K). Occasionally, faint staining was observed in the vascular tissues of cotyledons, although this activity was inconsistent (approximately 30% of observed seedlings). In mature *AtPERK3* promoter::GUS transgenic plants, rosette leaves consistently showed staining in the primary vein of the blade with inconsistent, and progressively less intense staining evident in secondary and higher order veins (Fig. 6L). In addition, faint GUS expression was evident in hydathodes of mature rosette leaves (Fig. 6L). Weak staining was also occasionally observed (approximately 50% of plants tested) in the central region of mature stems (Fig. 6M). GUS activity in reproductive organs was largely confined to developing and mature pollen grains (Fig. 6N and O).

DISCUSSION

In this study, we have begun a functional analysis of the PERKs in *Arabidopsis* using a variety of transgenic approaches. Analyses of transgenic *Arabidopsis thaliana* plants harboring the *BnPERK1* cDNA in either the sense or antisense orientations resulted in pleiotropic effects on the growth and development of *Arabidopsis*. In the antisense *BnPERK1* transgenic plants, developmental defects were observed in four independent lines resulting from the strong suppression of *AtPERK1*, and 3 as well as the partial suppression of *AtPERK6*, 7 and 13. These defects included reduced height and loss of apical dominance as well as abnormal flowers. Additional defects in the antisense *BnPERK1* transgenic *Arabidopsis* lines, AS35 and AS37, such as the reduced fertility may be attributed to increased suppression of different *PERK* genes in these tissues.

Ectopic expression of *BnPERK1* resulted in a significant increase in the number of ovules/pistil (and seeds/silique) as well as increased growth of the plant as a whole probably due to the prolonged lifespan. The ectopic *BnPERK1* lines also display some contrasting phenotypes to the antisense *BnPERK1* transgenic lines. In comparison to wild-type plants, the ectopic *BnPERK1* transgenic lines showed an increase in height, while the antisense *BnPERK1* transgenic lines were shorter in stature. All transgenic lines had an increase in the number of lateral shoots, but the mechanism appeared to be different according to our observations. The increased number of lateral shoots for the antisense *BnPERK1* transgenic lines was reminiscent of a reduced apical dominance.⁴¹ The ectopic *BnPERK1* transgenic lines took longer to senesce and produced more lateral shoots perhaps as a result of a prolonged lifespan rather than due to reduced apical dominance.

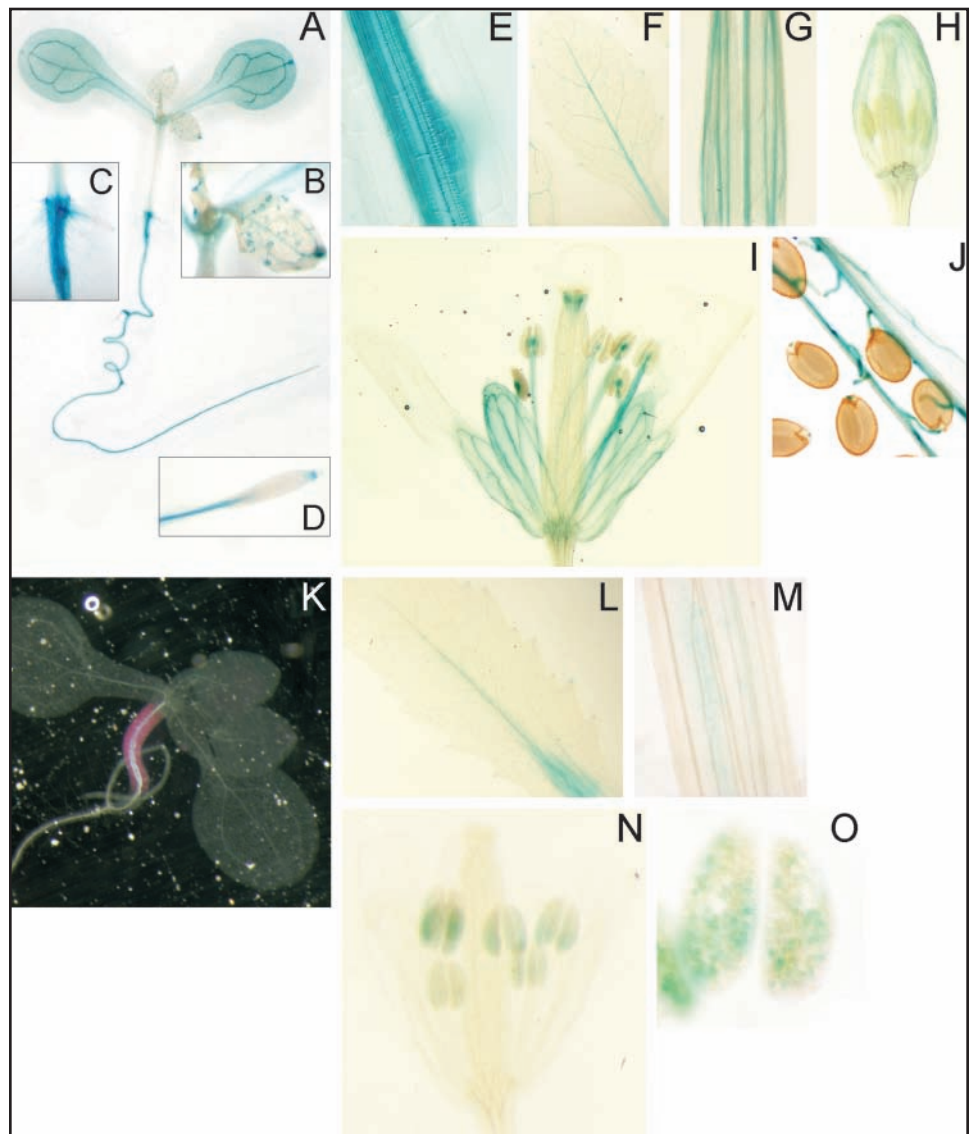


Figure 6. Histochemical localization of *AtPERK1* and *AtPERK3* promoter::GUS expression in *Arabidopsis*. (A to J) *AtPERK1* promoter::GUS expression: 7 day-old seedling showing (A) whole seedling, (B) first leaf, (C) hypocotyl-root junction and (D) root tip; (E) lateral root primordium; (F) rosette leaf; (G) stem segment from middle section of stem; (H) unopen flower bud; (I) open flower; (J) silique. (K to O) *AtPERK3* promoter::GUS expression: (K) dark field image of a 21 day-old seedling (GUS staining is seen as pink); (L) rosette leaf; (M) stem segment from middle section of stem; (N) open flower; (O) mature anthers containing pollen grains. Representative images are shown, following the analyses of multiple samples from at least two independent transgenic lines for both the *AtPERK1* and 3 promoters.

Furthermore, ectopic expression of *BnPERK1* resulted in increased numbers of ovules/pistil while the antisense suppression of *AtPERK1* and 3 led to abnormal flowers and siliques suggesting an important role for PERKs in floral organ formation and ovule number. Finally, there were changes in overall hypocotyl length and hypocotyl cell length in the transgenic lines, such that ectopic expression lines displayed decreased hypocotyl cell length while antisense lines tended to show some increase in hypocotyl cell length. This suggests that PERKs are involved in the regulation of the hypocotyl cell elongation.

Interestingly, ectopic callose and cellulose deposits were observed in the *BnPERK1* transgenic lines. Altered deposition of cell wall material can be indicative of cell wall changes,⁴⁶ and suggests that PERKs may have some type of regulatory role associated with cell wall biogenesis. This makes sense in light of the fact that the predicted

PERK extracellular domain is similar to cell wall proteins. The changes in hypocotyl cell elongation link nicely with such a proposed role where cell wall biogenesis is an integral part of cell elongation. Overall, however, the range of defects in these transgenic plants suggests that multiple developmental processes are affected.

The *AtPERK1*, and 3 promoter::GUS analyses revealed that these promoters drive expression predominantly in the vasculature, with the *AtPERK1* promoter being expressed in the vasculature throughout the plant. It is interesting to note that there was an absence of GUS activity in the division zone of the *AtPERK1* Promoter::GUS roots, with expression being found in rest of the root where cells would be undergoing elongation and differentiation. This would be consistent with a potential role for PERKs in cell elongation. However, it is rather difficult to reconcile some of these expression patterns with the range of phenotypic defects observed in the *BnPERK1* transgenic *Arabidopsis* lines, and a tentative regulatory role in the cell wall. One possibility is that the cell wall changes associated with altered PERK expression may result in secondary effects leading to the observed phenotypes. For example, subtle changes in the vascular tissues might affect the movement of plant growth regulators in the *Arabidopsis* plant. For example, the antisense *BnPERK1* transgenic *Arabidopsis* plants display classical auxin mutant phenotypes with the reduced apical dominance and increased shoot branching.⁴¹ In addition, the analyses of a number of different mutants involved in auxin transport or responses have indicated that auxin polar transport is important for the development of floral organs with a range of floral defects identified in these mutants.⁴⁷⁻⁵⁰

We have also analyzed *Arabidopsis* mutant lines carrying T-DNA insertions in each of the *AtPERK* genes.⁵¹ Individual *AtPERK* insertion lines do not display any detectable phenotypes suggesting that there is functional redundancy in this family (data not shown), where loss of one *AtPERK* can be partially compensated by another *AtPERK* with overlapping expression patterns and ligand-binding specificities. These lines are currently being crossed to generate plants carrying multiple *AtPERK* T-DNA insertions to examine the effects of disrupting multiple *AtPERK* genes. However, since the *AtPERK1* (*At3g24550*) and *AtPERK3* (*At3g24540*) genes are tandemly-linked, it will not be possible to generate *Arabidopsis* plants carrying T-DNA insertions in both of these two genes. Thus, one significant aspect of the antisense suppression results presented in this study is that the effects of suppressing both *AtPERK1* and 3 was examined. Evaluating the effects of suppressing other *AtPERK* members, and investigating possible associations with the cell wall are important areas for future investigation.

Acknowledgements

We are grateful to S. Tanaka for technical assistance, S. Cutler for access to his confocal microscope, B. Lam for experimental advice, and R. Serrano for the H⁺-ATPase antibody. We also thank T. Humphrey for critical reading of the manuscript. This work was supported by grants from the Natural Sciences and Engineering Research Council of Canada (NSERC) to D.R.G. and R.K.C., by Ontario Premier's Research Excellence Awards to D.R.G. and R.K.C., an Ontario graduate scholarship in Science & Technology to N.F.S., and an NSERC graduate scholarship to S.S.

References

- Haffani YZ, Silva NF, Goring DR. Receptor kinase signalling in plants. *Can J Bot* 2004; 82:1-15.
- Torii KU. Leucine-rich repeat receptor kinases in plants, structure, function, and signal transduction pathways. *Int Rev Cytol* 2004; 234:1-46.
- Shiu SH, Bleeker AB. Receptor-like kinases from *Arabidopsis* form a monophyletic gene family related to animal receptor kinases. *Proc Natl Acad Sci USA* 2001; 98:10763-8.
- Shiu SH, Bleeker AB. Plant receptor-like kinase gene family, diversity, function, and signaling. *Science STKE* 2001; 113:RE22.
- Shiu SH, Bleeker AB. Expansion of the receptor-like kinase *Pelle* gene family and receptor-like proteins in *Arabidopsis*. *Plant Physiol* 2003; 132:530-43.
- Shiu SH, Karlowski WM, Pan R, Tzeng YH, Mayer KF, Li WH. Comparative analysis of the receptor-like kinase family in *Arabidopsis* and rice. *Plant Cell* 2004; 16:1220-34.
- Cano-Delgado A, Yin Y, Yu C, Vafeados D, Mora-Garcia S, Cheng JC, Nam KH, Li J, Chory J. BRL1 and BRL3 are novel brassinosteroid receptors that function in vascular differentiation in *Arabidopsis*. *Development* 1998; 131:5341-51, (2004).
- Dievart A, Dalal M, Tax FE, Lacey AD, Hurlly A, Li J, Clark SE. CLAVATA1 dominant-negative alleles reveal functional overlap between multiple receptor kinases that regulate meristem and organ development. *Plant Cell* 2003; 15:1198-211.
- Shpak ED, Lakeman MB, Torii KU. Dominant-negative receptor uncovers redundancy in the *Arabidopsis* ERECTA Leucine-rich repeat receptor-like kinase signaling pathway that regulates organ shape. *Plant Cell* 2003; 15:1095-110.
- Shpak ED, Berthiaume CT, Hill EJ, Torii KU. Synergistic interaction of three ERECTA-family receptor-like kinases controls *Arabidopsis* organ growth and flower development by promoting cell proliferation. *Development* 2004; 131:1491-501.
- Zhou A, Wang H, Walker JC, Li J. BRL1, a leucine-rich repeat receptor-like protein kinase, is functionally redundant with BRI1 in regulating *Arabidopsis* brassinosteroid signaling. *Plant J* 2004; 40:399-409.
- Li J, Chory J. A putative leucine-rich repeat receptor kinase involved in brassinosteroid signal transduction. *Cell* 1997; 90:929-38.
- Li J, Wen J, Lease KA, Doke JT, Tax FE, Walker JC. BAK1, an *Arabidopsis* LRR receptor-like protein kinase, interacts with BRI1 and modulates brassinosteroid signaling. *Cell* 2002; 110:213-22.
- Nam KH, Li J. BRI1/BAK1, a receptor kinase pair mediating brassinosteroid signaling. *Cell* 2002; 110:203-12.
- Clark SE, Williams RW, Meyerowitz EM. The *CLAVATA1* gene encodes a putative receptor kinase that controls shoot and floral meristem size in *Arabidopsis*. *Cell* 1997; 89:575-85.
- Takasaki T, Hatakeyama K, Suzuki G, Watanabe M, Isogai A, Hinata K. The *S* receptor kinase determines self-incompatibility in *Brassica* stigma. *Nature* 2000; 403:913-6.
- Andre G, Kereszt A, Kevei Z, Mihacea S, Kalo P, Kiss GB. A receptor kinase gene regulating symbiotic nodule development. *Nature* 2002; 417:962-6.
- Stracke S, Kistner C, Yoshida S, Mulder L, Sato S, Kaneko T, Tabata S, Sandal N, Stougaard J, Szczyglowski K, Parniske M. A plant receptor-like kinase required for both bacterial and fungal symbiosis. *Nature* 2002; 417:959-62.
- Limpens E, Franken C, Smit P, Willemsse J, Bisseling T, Geurts R. LysM domain receptor kinases regulating rhizobial Nod factor-induced infection. *Science* 2003; 302:630-3.
- Madsen EB, Madsen LH, Radutoiu S, Olbryt M, Rakwalska M, Szczyglowski K, Sato S, Kaneko T, Tabata S, Sandal N, Stougaard J. A receptor kinase gene of the *LysM* type is involved in legume perception of rhizobial signals. *Nature* 2003; 425:637-40.
- Radutoiu S, Madsen LH, Madsen EB, Felle HH, Umehara Y, Gronlund M, Sato S, Nakamura Y, Tabata S, Sandal N, Stougaard J. Plant recognition of symbiotic bacteria requires two LysM receptor-like kinases. *Nature* 2003; 425:585-92.
- Song WY, Wang GL, Chen LL, Kim HS, Pi LY, Holsten T, Gardner J, Wang B, Zhai WX, Zhu LH, Fauquet C, Ronald P. A receptor kinase-like protein encoded by the rice disease resistance gene, *Xa21*. *Science* 1995; 270:1804-6.
- Gomez-Gomez L, Boller T. FLS2, an LRR receptor-like kinase involved in the perception of the bacterial elicitor flagellin in *Arabidopsis*. *Mol Cell* 2000; 5:1003-11.
- Pilling E, Hofte H. Feedback from the wall. *Curr Op Plant Biol* 1991; 6:611-616, (2003).
- Somerville C, Bauer S, Brininstool G, Facette M, Hamann T, Milne J, Osborne E, Paredes A, Persson S, Raab T, Vorwerk S, Youngs H. Toward a systems approach to understanding plant cell walls. *Science* 2004; 306:2206-11.
- He ZH, Fujiki M, Kohorn BD. A cell wall-associated, receptor-like protein kinase. *J Biol Chem* 1996; 271:19789-93.
- Wagner TA, Kohorn BD. Wall-associated kinases are expressed throughout plant development and are required for cell expansion. *Plant Cell* 2001; 13:303-18.
- Lally D, Ingmire P, Tong HY, He ZH. Antisense expression of a cell wall-associated protein kinase, WAK4, inhibits cell elongation and alters morphology. *Plant Cell* 2001; 13:1317-31.
- Decreux A, Messiaen J. Wall-associated kinase WAK1 interacts with cell wall pectins in a calcium-induced conformation. *Plant Cell Physiol* 2005; 46:268-78.
- Kohorn BD, Kobayashi M, Johansen S, Riese J, Huang LF, Koch K, Fu S, Dotson A, Byers N. An *Arabidopsis* cell wall-associated kinase required for invertase activity and cell growth. *Plant J* 2006; 46:307-16.
- Nakhmchik A, Zhao Z, Provart NJ, Shiu SH, Keatley SK, Cameron RK, Goring DR. A comprehensive expression analysis of the *Arabidopsis* proline-rich extensin-like receptor kinase gene family using bioinformatic and experimental approaches. *Plant Cell Physiol* 2004; 45:1875-81.

32. Cassab GI. Plant cell wall proteins. *Annu Rev Plant Physiol Plant Mol Biol* 1998; 49:281-309
33. Silva NE, Goring DR. The proline-rich, extensin-like receptor kinase-1 (*PERK1*) gene is rapidly induced by wounding. *Plant Mol Biol* 2002; 50:667-85.
34. Baumberger N, Ringli C, Keller B. The chimeric leucine-rich repeat/extensin cell wall protein LRX1 is required for root hair morphogenesis in *Arabidopsis thaliana*. *Genes Dev* 2001; 15:1128-39.
35. Baumberger N, Steiner M, Ryser U, Keller B, Ringli C. Synergistic interaction of the two paralogous *Arabidopsis* genes *LRX1* and *LRX2* in cell wall formation during root hair development. *Plant J* 2003; 35:71-81.
36. Clough SJ, Bent AF. Floral dip, a simplified method for *Agrobacterium*-mediated transformation of *Arabidopsis thaliana*. *Plant J* 1998; 16:735-43.
37. Nakazawa M, Matsui M. Selection of hygromycin-resistant *Arabidopsis* seedlings. *Biotechniques* 2003; 34:28-30.
38. Cock JM, Swarup R, Dumas C. Natural antisense transcripts of the S locus receptor kinase gene and related sequences in *Brassica oleracea*. *Mol Gen Genet* 1997; 255:514-24.
39. Larsson C, Sommarin M, Widell S. Isolation of highly purified plant plasma membrane and separating of inside-out and right-side-out vesicles. *Methods Enzymol* 1994; 228:451-69.
40. Stone SL, Arnoldo M, Goring DR. A breakdown of *Brassica* self-incompatibility in ARC1 antisense transgenic plants. *Science* 1999; 286:1729-31.
41. Lincoln C, Britton JH, Estelle M. Growth and development of the *axr1* mutants of *Arabidopsis*. *Plant Cell* 1990; 2:1071-80.
42. Kang J, Dengler N. Cell cycling frequency and expression of the homeobox gene *ATHB-8* during leaf vein development in *Arabidopsis*. *Planta* 2002; 216:212-9.
43. Shi H, Xiong L, Stevenson B, Lu T, Zhu JK. The *Arabidopsis* salt overly sensitive 4 mutants uncover a critical role for vitamin B6 in plant salt tolerance. *Plant Cell* 2002; 14:575-88.
44. von Heijne G. Membrane protein structure prediction. Hydrophobicity analysis and the positive-inside rule. *J Mol Biol* 1992; 225:487-94.
45. Schmid M, Davison TS, Henz SR, Pape UJ, Demar M, Vingron M, Scholkopf B, Weigel D, Lohmann JU. A gene expression map of *Arabidopsis thaliana* development. *Nature Genetics* 2005; 37:501-6.
46. Gillmor CS, Lukowitz W, Brininstool G, Sedbrook JC, Hamann T, Poindexter P, Somerville C. Glycosylphosphatidylinositol-anchored proteins are required for cell wall synthesis and morphogenesis in *Arabidopsis*. *Plant Cell* 2005; 17:1128-40.
47. Okada K, Ueda J, Komaki MK, Bell CJ, Shimura Y. Requirement of the Auxin polar transport system in early stages of *Arabidopsis* floral bud formation. *Plant Cell* 3:677-84.
48. Nemhauser JL, Feldman LJ, Zambryski PC. Auxin and ETTIN in *Arabidopsis* gynoecium morphogenesis. *Development* 2000; 127:3877-88.
49. Benjamins R, Quint A, Weijers D, Hooykaas P, Offringa R. The PINOID protein kinase regulates organ development in *Arabidopsis* by enhancing polar auxin transport. *Development* 2001; 128:4057-67.
50. Pfluger J, Zambryski P. The role of SEUSS in auxin response and floral organ patterning. *Development* 2004; 131:4697-707.
51. Alonso JM, Stepanova AN, Leisse TJ, Kim CJ, Chen H, Shinn P, Stevenson DK, Zimmerman J, Barajas P, Cheuk R, Gadrinab C, Heller C, Jeske A, Koesema E, Meyers CC, Parker H, Prednis L, Ansari Y, Choy N, Deen H, Geralt M, Hazari N, Hom E, Karnes M, Mulholland C, Ndubaku R, Schmidt I, Guzman P, Aguilar-Henonin L, Schmid M, Weigel D, Carter DE, Marchand T, Risseuw E, Brogden D, Zeko A, Crosby WL, Berry CC, Ecker JR. Genome-wide insertional mutagenesis of *Arabidopsis thaliana*. *Science* 2003; 301:653-7.